

Low mass ratio vortex-induced motion

B. Stappenbelt, F. Lalji and G. Tan

School of Mechanical Engineering
University of Western Australia, Perth, Western Australia, 6009 AUSTRALIA

Abstract

The vortex-induced motion of floating structures is strongly influenced by their low mass ratios (i.e. the ratio of structural to displaced fluid mass). It has previously been demonstrated that the super-upper response branch encountered in two-degree of freedom systems at low mass ratio is characterised by much larger vibration amplitudes than those of the corresponding upper response branch. These low mass ratio super-upper response branch vibrations are clearly of immense importance in the design and analysis of offshore structures. It was the purpose of the current study to experimentally investigate the vortex-induced response of cylindrical structures at low mass ratio with particular emphasis on the relative magnitude of the super-upper response branch vibration amplitudes. The experimental apparatus utilised, consisted of a parallel linkage mechanism allowing translation motion of the cylindrical test section in both the inline and transverse directions. The configuration employed ensured identical mass ratios and natural frequencies in both directions. The mass ratio range covered was nominally 2.4 to 13.

Introduction

Vortex-Induced Vibration (VIV) is a flow-structure interaction phenomenon in which the structure is excited by forces induced by vortices shed alternately from the edges of a bluff object. The time varying non-uniform pressure distribution around the object resulting from the vortex shedding (causing a time varying lift force to be experienced by the object) creates structural vibrations both inline and transverse to the flow. Near the natural frequency of the structure, the vortex shedding frequency synchronises with the natural frequency and the vibration frequency. One of the primary mechanisms responsible for this synchronisation is the change in hydrodynamic mass, as demonstrated in the experiments of Vikestad [18]. The range of reduced velocity over which this synchronisation occurs is known as the lock-in range. Mostly, the ensuing vibrations are undesirable, resulting in increased fatigue loading and component design complexity to accommodate these motions. The transverse vibrations also result in higher dynamic relative to static drag coefficients.

With decreasing mass ratio an increase in the amplitude response is generally evident [17]. Also, the smaller the mass ratio, the larger the relative influence of the hydrodynamic mass on the vibration response of the structure. Since the hydrodynamic mass variation is largely responsible for synchronisation of the shedding and vibration frequencies, typically much wider lock-in regions are experienced at low mass ratio [17]. The limit of this trend is found at the critical mass ratio of around 0.54 [4], below which, there exists no de-coherence region and VIV occurs at all velocities above the initial lock-in.

Various definitions for the mass ratio are widely employed. In the present work, the mass ratio is defined by the relationship

$$m^* = \frac{m}{m_f} \quad (1)$$

The denominator is the displaced fluid mass;

$$m_f = \rho L \pi \left(\frac{D^2}{4} \right) \quad (2)$$

The structural mass, m , includes enclosed fluid, but excludes the hydrodynamic mass. The term L is the submerged length of the cylinder. The mass ratio parameter is therefore the ratio of the oscillating structural mass to the displaced fluid mass. In the present study, the term low mass ratio refers to mass ratios of the order of one. These mass ratio magnitudes are common for marine structures.

The mass ratio parameter influences both the amplitude and frequency response of the cylinder. With higher mass ratios (e.g. a cylinder vibrating in air, with a mass ratio $O(100)$), changes in added mass are relatively insignificant due to the low density of the fluid. The natural frequency therefore, remains relatively unchanged throughout the lock-in range. When the fluid medium under consideration is much denser (e.g. a cylinder vibrating in water), distinct changes in the natural frequency are observed. The increasing natural frequency observed with increasing reduced velocity is directly attributable to the decreasing added mass throughout the lock-in range [16, 18].

The shedding of vortices from cylindrical bluff objects and the ensuing vibrations are well documented for single degree of freedom cases (see for example the review by Griffin [6]). Investigations tended to focus on the larger transverse vibrations and any interaction with the inline oscillations, which occur at twice the transverse vibration frequency, was ignored. Experimental investigations conducted by Williamson & Jauvtis [19] revealed the existence of a super-upper response branch when two degrees of freedom were considered. It was noted that these vibrations were extremely large and regular compared to those observed in the upper response branch. The regularity of these large-amplitude vibrations observed appear to indicate that the amplitude limitation due to disruption of the regular vortex shedding process (discussed in the text by Blevins [2]) is much more distinct in the two-degree of freedom than the single-degree of freedom upper response branch oscillations.

The super-upper response branch has also been observed in other investigations, such as the cantilevered cylinder experimental study by Pesce & Fujarra [12], the neutrally buoyant cylinder experiments by Hansen, Bryndum & Mayer [7] and the VIV work on non-linear compliant systems by Stappenbelt [16]. In the studies of Williamson & Jauvtis [19] and Stappenbelt [16], it was noted that the extremities of the super-upper response branch terminate at the single degree of freedom vortex-shedding mode boundaries. The vortex shedding mode observed during the super-upper response branch vibrations are an alternating pair of

triple vortices (referred to as the 2T mode) as opposed to the 2P (i.e. pairs of vortices) mode observed in the upper response branch. As in the single degree of freedom case, the initial response branch is still characterised by the classic von Karman 2S shedding mode in the two degree of freedom case.

The studies of Jauvtis & Williamson [8, 9] arrived at the conclusion that for mass ratios above five or six, there was no significant change in the transverse oscillatory response from one to two degrees of freedom. This mass ratio boundary delineating the presence of the super-upper response branch was reported at a mass ratio of approximately 8.5 in the study of Stappenbelt and O’Neill [15]. These findings of course have potential bearing on the validity of the volumes of single degree of freedom VIV data employed in multiple degree of freedom system design situations. As suggested by Jauvtis & Williamson [9], offshore design codes should reflect the significant deviation from the single degree of freedom VIV data when dealing with the low mass ratios typically encountered in offshore structure design.

Methodology

The experimental investigation conducted, examined the single (transverse motion only) and two-degree of freedom VIV response of an elastically mounted rigid cylinder with low mass ratio under steady, uniform current conditions. The apparatus utilised consisted of a towing carriage and a parallel linkage mechanism capable of translation motion in the transverse and inline directions (the mechanism is illustrated in figures 1 and 2).

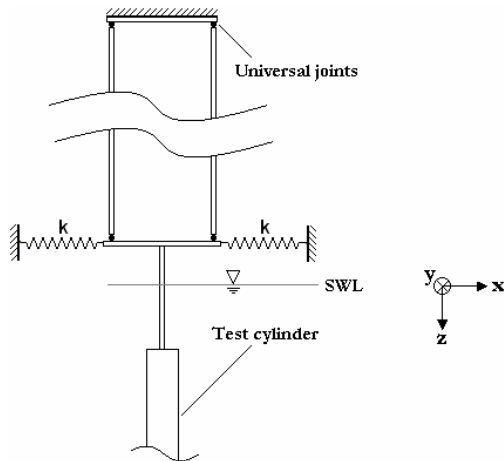


Figure 1 – Elevation view of the two degree of freedom experimental apparatus

The mechanism employed ensured identical mass ratios and natural frequencies in both directions. Inline motion was restricted for the transverse VIV only part of the experiment, through the use of diagonal cross braces between linkages. To avoid influencing the cylinder effective mass, the braces remained attached to the linkages for all experimentation. Experimental parameter values utilised in the present investigation are listed in table 1.

The apparatus for the experiment was lightly damped at around 0.6% of the critical damping. Damping ratios were effectively constant over the experimental amplitude response range. At very small vibration amplitudes however, the damping ratio increased marginally due to the effect of initial static frictional component in the universal joints employed. This low amplitude damping ratio increase did not extend to the vibration amplitudes experienced in the upper and super-upper response branches of interest in the present study.

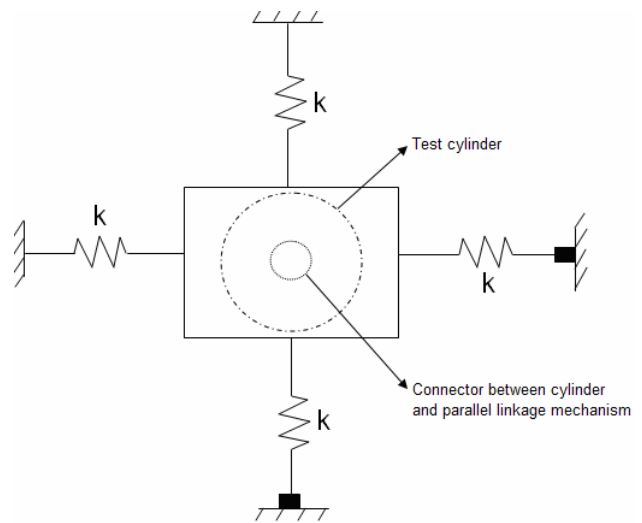


Figure 2 – Plan view of the two degree of freedom experimental apparatus

The mass ratio range covered was 2.36 to 12.96. This was achieved through the addition of lump masses to the plate attaching the cylinder test section to the parallel linkages. The test section support had an effective stiffness three orders of magnitude higher than that imposed by the linear coiled tension spring arrangement.

Table 1– Experimental parameters.

Parameter	Symbol	Value	Units
Cylinder diameter	D	0.0554	m
Cylinder length	L	0.4432	m
Normalised parallel linkage length	l/D	12.27	
Cylinder mass (incl. enclosed fluid) ¹	m	2.53	kg
System stiffness	k_1	453.0	N/m
Damping ratio	ζ	0.006	
Natural frequency in air ¹	ω_v	16.32	rad/s
Still-water natural frequency ¹	ω_{ov}	10.75	rad/s
Mass ratio range	m^*	2.36-12.96	-

¹Cylinder only (i.e. base case without lump masses attached).

Throughout the present study, the flow velocities are presented normalised (i.e. as reduced velocities, U_r) by the product of the cylinder diameter and the natural frequency of the structure in still-water. The natural frequencies in still water (table 2) of the various mass ratios examined were determined through free-decay tests.

Table 2 – Natural frequencies in still-water

m^*	$m^*\zeta$	f_n (Hz)	ω_n (rad/s)
2.36	0.014	1.711	10.75
3.68	0.022	1.502	9.44
5.19	0.031	1.359	8.54
6.54	0.039	1.261	7.92
7.91	0.047	1.153	7.25
8.76	0.053	1.151	7.23
10.63	0.064	1.084	6.81
12.96	0.078	1.025	6.44

To simulate steady, uniform current conditions the structure was towed through initially still water. The ratio of cylinder diameter to channel width was 1:25 (representing around 1% of the channel area). No significant variation in local current velocity

due to blockage effects was therefore experienced. All experimentation was conducted within the stable subcritical Reynolds number range and only smooth cylinders were considered.

The cylinder aspect ratio was selected to bring the test section closer to commonly employed cylindrical floating structure ratios of around 3 to 5. The experiment did not employ test section end-plates. The influence of the end-conditions on the cylinder forcing at this small aspect ratio are likely therefore to have resulted in lowered excitation frequencies. Strouhal number and vortex shedding frequency data are traditionally collected with very large aspect ratios ($L/D \gg 100$) and commonly, using the walls of the tank effectively as very large end-plates (maintaining two-dimensional flow at the cylinder ends). A number of studies have shown a decrease in the shedding frequency with decreasing aspect ratio. Examples include the low Reynolds number study of Lee & Budwig [10] and the higher Reynolds number study of Gowda [5].

Experimentation and analysis of previous work by Gerich & Eckelman [3] demonstrated regions near the cylinder ends where the shedding frequency was significantly lower (up to a reported 17% below the Strouhal frequency). Below an aspect ratio of approximately 15, the shedding frequency is dominated by these regions (i.e. the shedding is controlled by the end conditions). Further examination of the effect of the end-conditions (with Reynolds numbers up to 10^4) on vortex shedding by Norberg [11], also demonstrated a decreased shedding frequency with reduced end-plate size. In the limit of this trend is of course the present case of a cylinder without end-plates.

In the present study, the cylinder was non surface-piercing and the top cylinder end was at a distance $4D$ below the free surface. No compensating corrections were applied for the surface proximity or to account for the small hydrodynamic forces acting on the rectangular cylinder support structure. Of interest in the present experiment, were the cylinder displacement, acceleration and hydrodynamic forces. Both magnitude and spectral information was extracted from the data. The cylinder inline and transverse force measurements were inertially corrected to yield the fluctuating drag and lift forces respectively. Spectral force information was used to ascertain the vortex-shedding frequency also. For further details regarding the experimental arrangement, the reader is directed to the doctoral thesis by Stappenbelt [16].

The primary aim of the present study was to determine the point at which the variation between the single and two-degree of freedom transverse amplitude responses becomes significant. As applied in the studies by Jauvtis & Williamson [8, 9], the governing parameter was assumed to be the mass ratio. The point of prime experimental interest was therefore the upper mass ratio limit where the super-upper response branch was discernible on the transverse amplitude plot of both the single and two-degree of freedom data.

Results

Examples of the single and two-degree of freedom vortex-induced vibration time series are presented in figures 3 and 4. The cases illustrated are at a reduced velocity of seven, at the lowest mass ratio examined ($m^* = 2.36$). These examples were selected to illustrate the difference in cylinder response in the super-upper and upper response branches.

A noteworthy feature of these time series is the relative regularity of the transverse motion maxima in the two-degree of freedom situation. The large amplitude and regularity of vibration of the super-upper response (figure 4) are evident when compared to the

upper branch response (figure 3). These are characteristic features of the super-upper response branch.

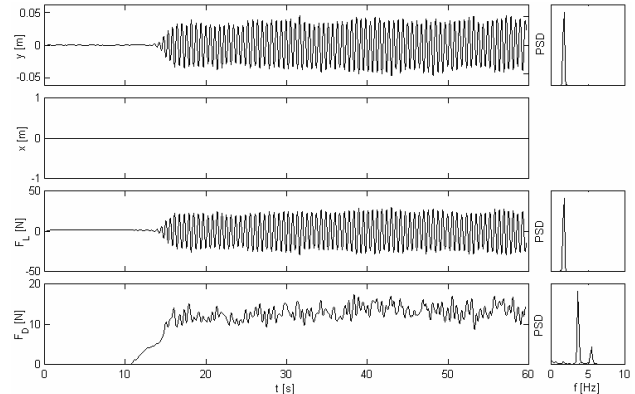


Figure 3 – Time series; $m^* = 2.36$, $U_r = 7$, 1 dof.

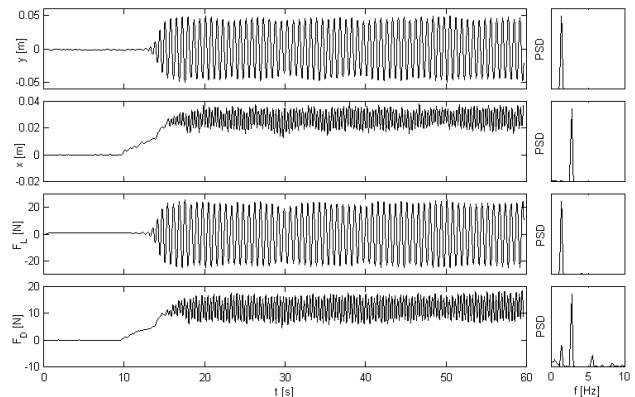


Figure 4 – Time series; $m^* = 2.36$, $U_r = 7$, 2 dof.

The transverse vibration maximum amplitude response plots for each of the mass ratios covered are presented in figures 5a through to 5h. The maximum amplitude was defined as the mean of the top 10% of half peak to peak values. As expected, the lock-in range was wider with lower mass ratio. Distinct shifts of the lock-in point to higher reduced velocities and a shift in the lock-out point toward lower reduced velocity were observed at the higher mass ratios. There also exists a slight shift in the corresponding transverse amplitude maxima to higher reduced velocities with increasing mass ratio in the two-degree of freedom case. This trend was not present in the single-degree of freedom case. Also evident from figure 5 is the expected decrease in response amplitude with increasing mass ratio for both the single and two degree of freedom cases. Notably, the decrease was more pronounced for the two-degree of freedom case.

With the single and two-degree of freedom data presented on the same axes, the super-upper response branch is clearly discernible as a deviation between the plots. Note the distinct jump, in the low mass ratio cases, at the upper end of the super-upper response branch back to the lower response branch.

The difference in maximum amplitudes of the single and two-degree of freedom responses decrease with increasing mass ratio. There appears to be a gradual alignment of the two-degree of freedom vibrations and the transverse motion only case with increasing mass ratio. At $m^* = 10.63$ there is general agreement of the two cases (less than 2.5% variation between the peaks of the response plots). At $m^* = 12.96$, this agreement is within 1.5%. The initial and lower response branches at all mass ratios are essentially identical for the single and two degree of freedom cases as is the de-coherence region post lock-in.

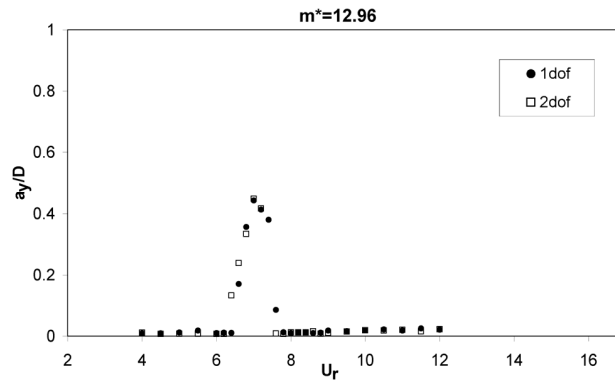
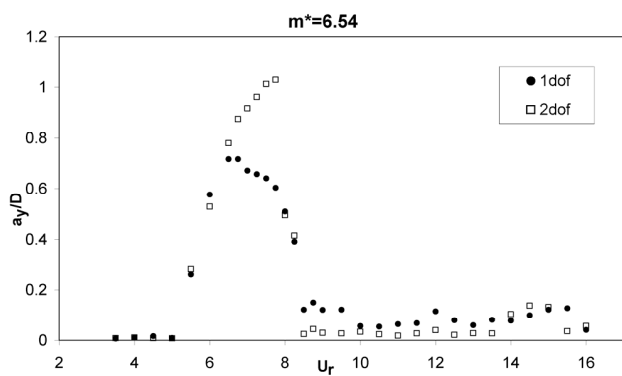
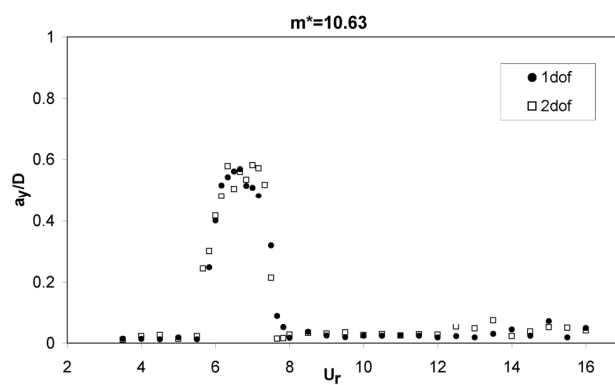
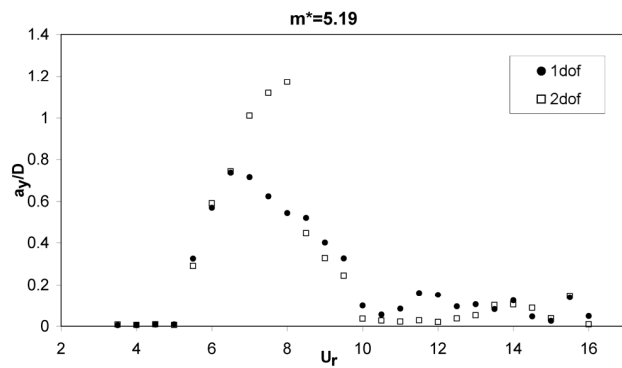
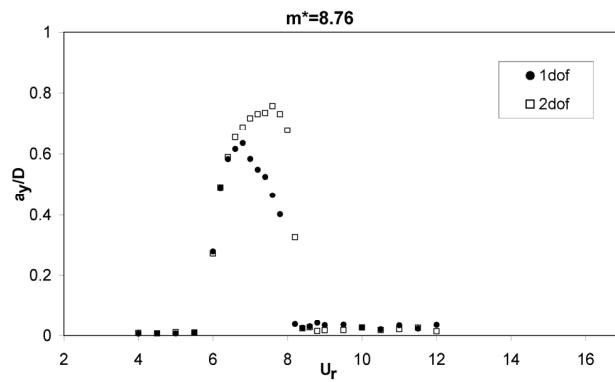
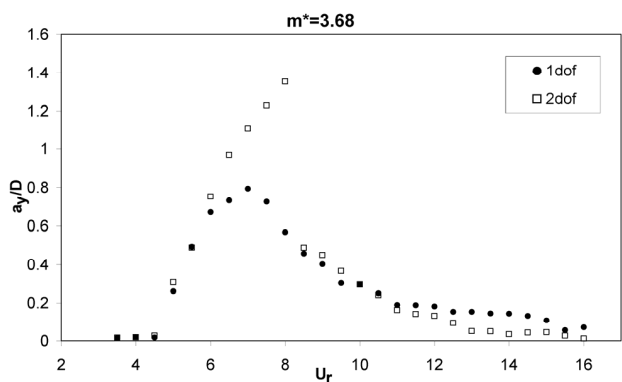
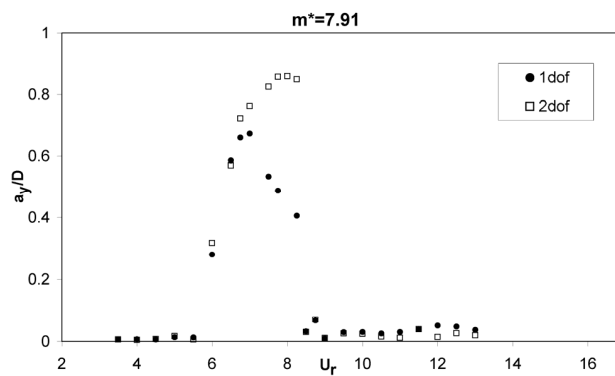
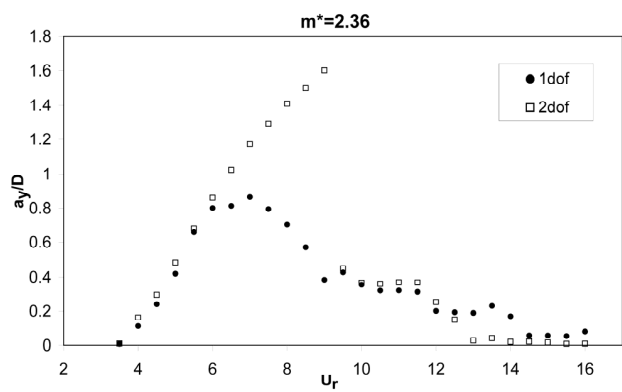


Figure 5 – Transverse response amplitude single and two-degree of freedom; a) $m^*=2.36$, b) $m^*=3.68$, c) $m^*=5.19$, d) $m^*=6.54$, e) $m^*=7.91$, f) $m^*=8.76$, g) 10.63 and h) $m^*=12.96$.

The inline response amplitude (figure 6) follows the same trend as the transverse response amplitude with respect to maximum vibration amplitude (i.e. decreased maxima with increasing mass ratio). The range of the amplitude response region for the inline vibrations also widens with decreasing mass ratio. The inline response peaks align best with the two degree of freedom maxima rather than the single degree of freedom maxima as was observed in the work of Stappenbelt [16] and the review by Sarpkaya [14].

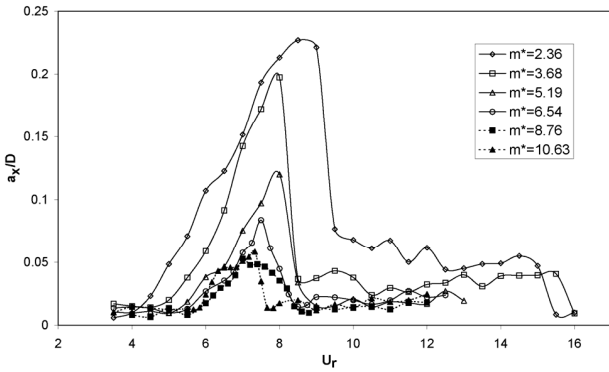


Figure 6 – Inline response amplitude

Examination of the vortex-shedding and vibration frequencies at each mass ratio reinforce the prior observations regarding the range of the amplitude response region. Figures 7 and 8 illustrate the $m^*=2.36$ case and figures 9 and 10 the $m^*=10.63$ case. The lock-in region is defined by the coincident vortex shedding and cylinder transverse vibration frequencies.

Synchronisation of the vortex-shedding and vibration frequencies begins at lower reduced velocity and extends to higher reduced velocity for the lower mass ratio cases (see table 3). No significant difference is noted in the lock-in region for the single and two-degree of freedom cases. The lock-in range remained essentially unaltered from one to two degrees of freedom regardless of whether the super-upper or upper response branch was present. This is not unexpected in light of the previously discussed observations regarding the vortex-shedding mode boundaries of the super-upper response branch. It is also consistent with the observation that the initial and lower response branches are essentially identical for the single and two degree of freedom cases since the extremities of these branches delineate the lock-in and lock-out points.

Table 3 – Lock-in values

m^*	dof	Initial lock-in (U_r)	Lock-in range (ΔU_r)
2.36	1	4.0	8.5
3.68	1	5.0	7.0
5.19	1	5.5	5.0
6.54	1	5.5	4.5
7.91	1	5.5	3.5
8.76	1	5.5	2.7
10.63	1	5.8	2.0
12.96	1	6.4	1.4

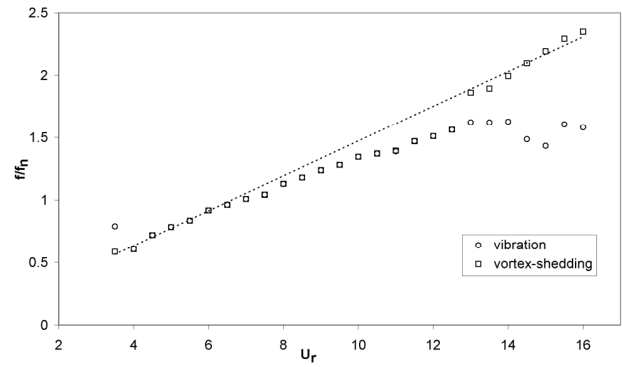


Figure 7 – Vibration and vortex shedding frequencies; $m^*=2.36$, 1 dof.

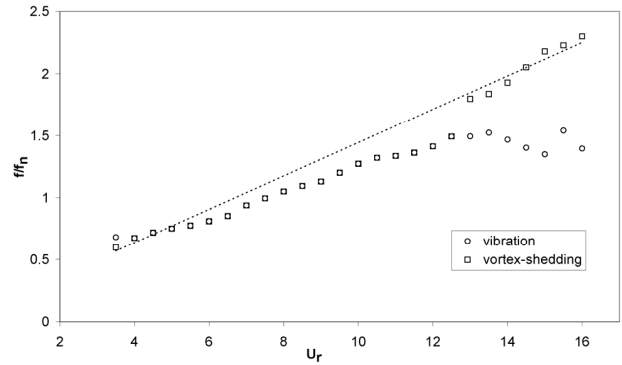


Figure 8 – Vibration and vortex shedding frequencies; $m^*=2.36$, 2 dof.

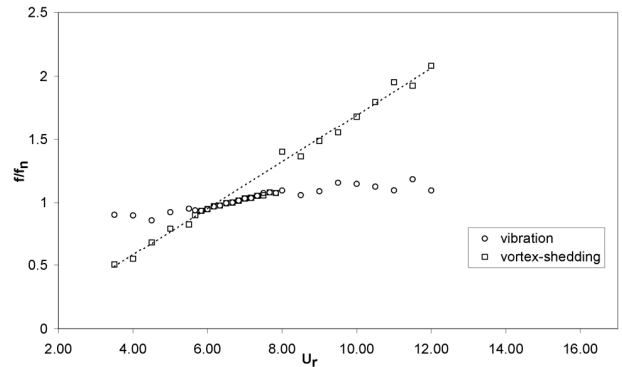


Figure 9 – Vibration and vortex shedding frequencies; $m^*=10.63$, 1 dof.

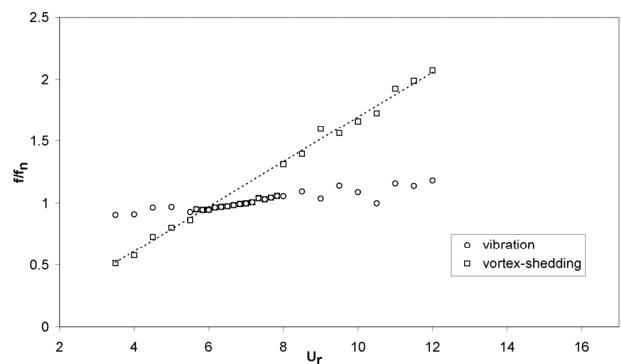


Figure 10 – Vibration and vortex shedding frequencies; $m^*=10.63$, 2 dof.

Table 4 lists the Strouhal frequencies for all cases covered with the corresponding index of fit. As expected, the Strouhal frequencies are significantly lower than the commonly reported values of around 0.2 to 0.21 [17] due to the previously discussed effects related to the low aspect ratio of the cylinder and the lack of cylinder end-plates.

It must be noted at this point that since the cylinder is not stationary at any towing velocity over the experimental range, the shedding frequencies pre and post lock-in allow for the determination of estimates of the Strouhal frequency only. From table 4, it may be noted that the Strouhal estimates for each mass ratio are not identical. This would appear to indicate that the vibration and shedding frequencies outside the lock-in range still influence one another. The observed trend was one of lowered Strouhal frequency with decreasing mass ratio.

Table 4 – Strouhal frequencies

m^*	dof	St	R^2
2.36	1	0.140	0.995
3.68	1	0.145	0.997
5.19	1	0.155	0.994
6.54	1	0.166	0.998
7.91	1	0.176	0.996
8.76	1	0.180	0.996
10.63	1	0.186	0.995
12.96	1	0.198	0.991

Prior experimentation [2, 13] purports the existence of a linear relationship between the mean drag and the transverse oscillation amplitude of the form

$$\bar{C}_d = \bar{C}_{d0} \left[1 + \kappa \left(\frac{a_y}{D} \right) \right]. \quad (3)$$

The experimentally determined curve fit parameter, κ , has been reported at around 2 [13] and 2.1 [2] for single degree of freedom cases. The curve fit parameters for the present study are presented in table 5. As noted in the study by Stappenbelt [16], the two-degree of freedom gradient is lower than that observed in the single degree of freedom case. The stationary cylinder drag coefficients match the aspect ratio adjusted fixed-cylinder drag data of Achenbach [1] reasonably well.

Table 5 – Mean drag coefficient as a function of transverse displacement amplitude for $m^*=2.36$.

Degrees of freedom	κ	\bar{C}_{d0}	R^2
1	1.80	0.75	0.92
2	1.34	0.83	0.97

The super-upper response branch and the corresponding mass ratio limit are also discernible from the drag coefficient plots. Figures 11 to 14 illustrate the gradual coalescing of the drag coefficient plots for the single and two-degree of freedom cases with increasing mass ratio as observed with the transverse response amplitude plots.

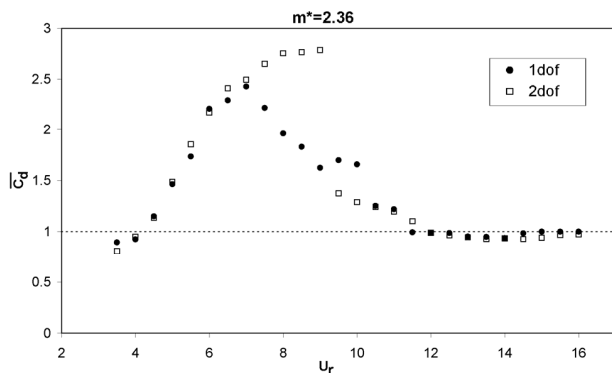


Figure 11 – Mean drag coefficients; $m^*=2.36$.

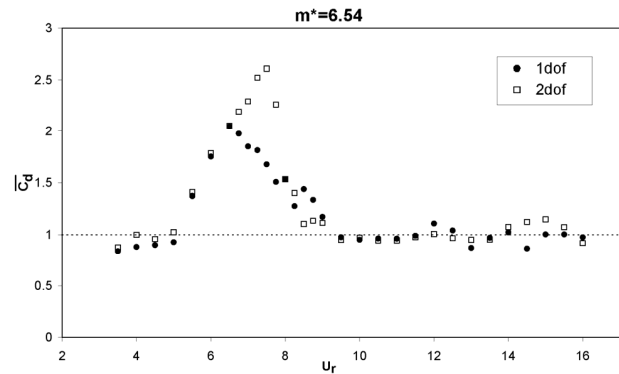


Figure 12 – Mean drag coefficients; $m^*=6.54$.

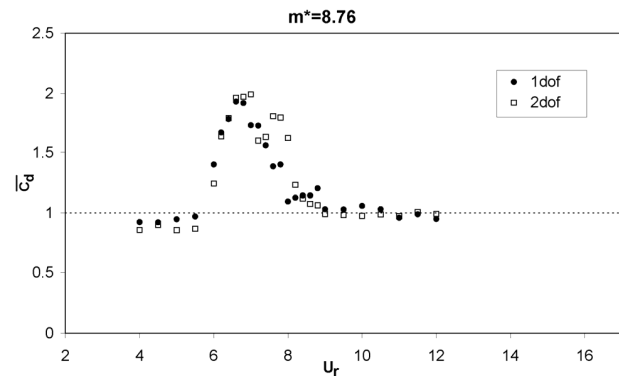


Figure 13 – Mean drag coefficients; $m^*=8.76$.

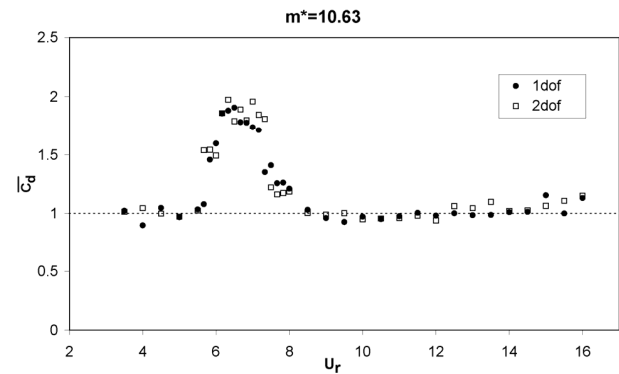


Figure 14 – Mean drag coefficients; $m^*=10.63$.

Conclusions

Consistent with prior studies, a widening of the lock-in region and increased transverse response amplitudes are observed with decreasing mass ratio. The increasing influence of the hydrodynamic mass at low mass ratio is largely responsible for the changes in the lock-in region. The decrease in transverse amplitude response magnitude with increasing mass ratio was more pronounced with two degrees of freedom.

The present study provides evidence consistent with the existence of the super-upper response branch in two-degree of freedom low mass ratio systems. The super-upper response branch was clearly observable in the two degree of freedom cases up to a mass ratio of 8.76. At the mass ratio of 10.63 the single and two-degree of freedom transverse amplitude response plots peak align to within 2.5%. The alignment does not present as an abrupt change, but rather a gradual coalescing of the single and two-degree of freedom system responses with increasing mass ratio as illustrated in figure 15.

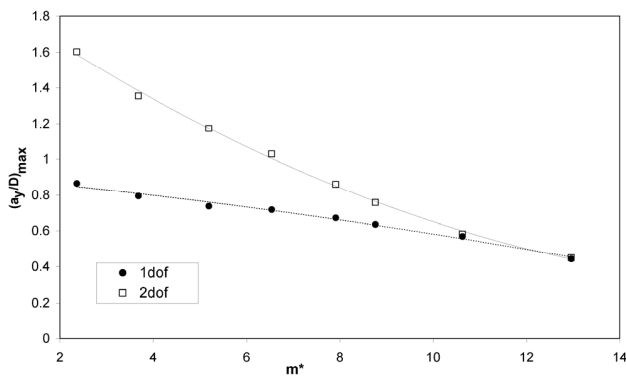


Figure 15 – Transverse response amplitude maxima.

The disparity between the present results and the prior work by Jauvtis & Williamson [9] regarding the upper mass ratio limit implies that the mass ratio may not be the sole determining parameter in the prediction of the occurrence of the super-upper response of a cylinder undergoing VIV. The difference in the results reported by Jauvtis & Williamson [9] and the present study may in part be due to the order of magnitude variation in structural damping ratio. The present study, with the higher damping ratio displayed the alignment between single and two-degree of freedom cases at a higher mass ratio.

The authors are in agreement with the suggestion by Jauvtis & Williamson [9] that offshore design codes should reflect the significant deviation from the single degree of freedom VIV data when dealing with the low mass ratios typically encountered in offshore structure design. However, the mass ratio limit of the super-upper response branch reported in these studies does not appear to be a suitable conservative cut-off point (for the use of empirical relationships based upon single degree of freedom VIV data) in light of the present results. Further investigation is required before any conclusions may be reached regarding the boundaries of the occurrence of the super-upper response branch and the governing parameters so that these may be amalgamated into existing design methods.

Acknowledgments

The authors gratefully acknowledge the financial support of the University of Western Australia Faculty of Engineering, Computing and Mathematics Futures Foundation. The contribution of Shadi Rawas during the experimental work was also much appreciated.

References

[1] Achenbach, E., 1971, 'Influence of surface roughness on the cross-flow around a circular cylinder', *Journal of Fluid Mechanics*, 46:321-335.

[2] Blevins, R. D., 1990, 'Flow-Induced Vibration (Second ed.)', New York, USA: Van Nostrand Reinhold.

[3] Gerich, D. & Eckelman, H. 1982, "Influence of the end plates and free ends on the shedding frequency of circular cylinders", *Journal of Fluid Mechanics*, 122:109-121.

[4] Govardhan, R. & Williamson, C. 2003, 'Critical mass in vortex-induced vibration of a cylinder', *Journal of Mechanics B/Fluids*.

[5] Gowda, B. H. L. 1975 "Some measurements of the phenomena of vortex-shedding and induced vibrations of circular cylinders", Technical Report DLR-FB 75-01, Technische Univeritat ,Berlin.

[6] Griffin, O.M. 1985 'Vortex-Induced Vibrations of Marine Cables and Structures', Naval Research Laboratory - Marine Technology Division, Washington D.C.

[7] Hansen, E., Bryndum, M. & Mayer, S. 2002 'Interaction of in-line and cross-flow vortex-induced vibrations in risers', OMAE2002-28303, 21st International Conference on Offshore Mechanics and Arctic Engineering, Oslo, Norway.

[8] Jauvtis, N. & Williamson, C., 2003, 'Vortex-induced vibration of a cylinder with two degrees of freedom', *Journal of Fluids and Structures*, 17:1035-1042.

[9] Jauvtis, N. & Williamson, C., 2004, 'The effect of two degrees of freedom on vortex-induced vibration at low mass and damping', *Journal of Fluid Mechanics*, 509:23-62.

[10] Lee, T. & Budwig, R., 1991, "A study of the effect of aspect ratio on vortex shedding behind circular cylinders", *Physics of Fluids A*, 34:309-315.

[11] Norberg, C., 1994 "Experimental investigation of the flow around a circular cylinder: influence of aspect ratio", *Journal of Fluid Mechanics*, 258:287-316.

[12] Pesce, C. & Fujarra, A. 2005, 'The super-upper branch VIV response of flexible cylinders', BBVIV4, Conference on Bluff Body Wakes and Vortex-Induced Vibrations, Santorini, Greece.

[13] Sarpkaya, T. 1978, 'Fluid forces on oscillating cylinders', *Journal of the Waterway, Port, Coastal and Ocean Division, Proceedings of the American Society of Civil Engineers*, 104 4, pp. 275-290.

[14] Sarpkaya, T. 2004, 'A critical review of the intrinsic nature of vortex-induced vibrations', *Journal of Fluids and Structures*, 19:389-447.

[15] Stappenbelt, B. & O'Neill, L. 2007, 'Vortex-Induced Vibration of Cylindrical Structures with Low Mass Ratio', ISOPE-JSC-292, 17th International Offshore and Polar Engineering Conference, Lisbon, Portugal.

[16] Stappenbelt, B. 2006, 'Vortex-Induced Vibration of Moored Cylindrical Structures', PhD Thesis, The University of Western Australia.

[17] Sumer, B. M. & Fredsoe, J., 1997, 'Hydrodynamics around Cylindrical Structures', World Scientific Publishing Co. Pte. Ltd., London.

[18] Vikestad, K. 1998, 'Multi-frequency response of a cylinder subjected to vortex shedding and support motions', PhD Thesis, Norwegian University of Science and Technology, Trondheim, Norway.

[19] Williamson, C. & Jauvtis, N., 2004, 'A High-Amplitude 2T Mode of Vortex-Induced Vibration for a Light Body in XY Motion', *European Journal of Mechanics B/Fluids* 23, 107-114.

Author Index

- Ahmadzadegan A, 163
Ahmed S, 75
Al-Khamis JN, 531
Alam F, 324, 758, 762, 1411
Alamgholilou A, 671
Altenhofer P, 1171
Alvarez M, 621
Amir AF, 104
Anderson B, 1392
Andrewartha JM, 241
Antonia RA, 287, 914
Archer RA, 803
Arifin D, 621
Armfield S, 961
Armfield SA, 1427
Armfield SW, 125, 699, 771, 856, 1148
Ashna M, 671
Ashraf MA, 1283
Atkinson CH, 184, 191
Austin JM, 385
Ayello F, 531
Azhdarzadeh M, 836
Azhdarzadeh ZH, 836
- Badra J, 1187
Baheri S, 1033
Baldock TE, 939
Banerjee PK, 1042
Barber T, 414, 1266
Barber TJ, 328, 919
Barnes MP, 939
Barton AF, 819
Bednarz TP, 368, 1165
Behnia M, 1427
Benaissa A, 914
Beyghi F', 831
Bilger RW, 1344
Blackburn HM, 82, 411, 559
Blazweicz AM, 930, 935
Boretti AA, 1142
Boyce RR, 507
Brady PDM, 1071
Brandis A, 461
Brandis AM, 594
Brandner P, 819
Brandner PA, 630, 1381, 1392, 1399
Brear MJ, 99, 1142, 1340
Brennan MS, 1042, 1131
Brett JD, 257
- Broutman D, 947
Brovkin V, 199
Brown RJ, 180, 777, 815
Brown S, 527
Buchmann NA, 60, 1364
Buckett C, 1369
Bui A, 167, 515
Bull MK, 930, 935
Burattini P, 287, 991
Busch H, 1470
Buttsworth DR, 766, 825, 1258
- Carati D, 991
Carberry J, 1486
Castillo L, 279
Cave HM, 1026
Chai WS, 1291
Chanel PG, 1201
Chanson H, 39, 691
Chao DA, 279
Chen JH, 1271
Chen L, 573, 712, 1405, 1475
Chenoweth SKM, 151
Cheung CP, 1405
Chiesa M, 1154
Chin CC, 1436
Chng TS, 1481
Chong M, 266
Chong MS, 271, 559, 807
Chou SK, 59
Chowdhury K, 1356
Christo FC, 1158
Clarke DB, 1381
Cleary MJ, 551
Cleary PW, 253
Cole DE, 866
Collins MJ, 616
Connor JN, 638
Coussot P, 54
Crook S, 429
Cruz T, 531
- Dally BB, 1350
Dann AG, 1304
Das D, 984
Das R, 253
Davidson MR, 798
Davidson PA, 545
Davison C, 825
Dawson PD, 943

De Leebeeck A, 291
 Deev AV, 638, 1050
 Denier JP, 967
 Deo RC, 262
 Dillon-Gibbons CJ, 1249, 1475
 Djenidi L, 914
 Do TT, 573
 Doering JC, 1201
 Doherty J, 266
 Doolan CJ, 1095, 1432
 Dragomir SC, 1207
 Drobik J, 429
 Druskovich D, 638
 Duan WS, 225
 Duke D, 892
 Dunn MJ, 1344

 Easton C, 527
 Eckermann SD, 947
 Egerton JO, 777
 Eichmann T, 373
 Eichmann TN, 461
 El Hassan M, 421
 Elsinga GE, 729
 Erm LP, 381
 Eslami G, 831
 Eslamian A, 1420
 Esmaeilzadeh E, 671, 831, 1033

 Felder S, 691
 Fife P, 159
 Fitch M, 1187
 Fitzgerald MJ, 1055
 Freeman M, 1187
 Frendo M, 487
 Friend J, 621, 1038
 Friend JR, 625, 790, 794
 Fry M, 1131
 Fukuyama E, 180
 Fulford GR, 616

 Gaarder AH, 291
 Gai L, 1309
 Gallis RM, 943
 Galoul V, 919
 Gangurde DY, 645
 Gao Q, 135
 Garen W, 207
 Gaston M, 1071
 Gharraei R, 1033
 Ghosh S, 308, 1356
 Giacobello M, 677, 870
 Gillam N, 771

 Gilmore J, 436
 Gnoffo PA, 24
 Gollan RJ, 295, 373
 Gongora N, 466
 Gonzalez CA, 1148
 Gonzalez LF, 471
 Gounder JD, 519
 Gran IR, 862
 Gray D, 939
 Griffiths RW, 954
 Guard A, 939
 Guzzomi FG, 1123

 Hafez S, 995
 Haker B, 487
 Hanslow D, 939
 Haque SME, 1050
 Harvie DJE, 798
 Hassan ER, 142, 146, 967
 Hassan NMS, 1315
 Hawkes ER, 1271
 Haynes J, 1116
 Hem Lata W, 1388
 Henderson AD, 87, 1116
 Herpin S, 726, 737
 Hibiki T, 848
 Hie T, 939
 Hield PA, 99
 Higgins K, 608
 Ho-Minh D, 1321
 Hohmann A, 1171
 Holtham PN, 1042, 1131
 Honda T, 704
 Hong G, 887, 1236
 Honnery D, 217
 Hoshino T, 180
 Hosseinalipour SM, 971, 976
 Hourigan K, 346, 361, 580
 Hruschka R, 456
 Hua HW, 1102
 Hua ZL, 782
 Hughes GO, 954
 Hughes L, 233
 Hultmark M, 907
 Humble R, 729
 Hutchins N, 271, 807, 1442
 Hutli EA, 876, 881
 Huynh, 487
 Huynh BP, 654

 Iannuccelli M, 414
 Ichimiya M, 708
 Ilic V, 876, 881

Inthavong K, 68, 842
 Ivan C, 531

 Jacobs CM, 602
 Jacobs PA, 295, 373, 385, 594, 645
 Jafar F, 1193
 Jahangirian A, 475
 Jaitlee R, 762
 Jamison RA, 353
 Jeng DS, 1083
 Jermy M, 436, 1102
 Jermy MC, 60, 1026, 1364
 Jin SH, 1340
 Jing ZY, 782
 Johnston IA, 295
 Jones JR, 1158
 Jones MB, 616
 Jones RF, 684

 Kalt PAM, 1350
 Karimi N, 1340
 Kato C, 704
 Kato K, 1295
 Kavnoudias H, 75
 Keirsbulck L, 421
 Kelso R, 429
 Kelso RM, 142, 146, 930, 935, 967, 1003
 Kendall MAF, 613
 Khan M, 1411
 Khan MMK, 1050, 1315, 1369
 Khmara D, 199
 Kilany K, 712
 Kinet M, 991
 Kirchhartz RM, 491
 Kirkpatrick MP, 771, 1427
 Kitsios V, 892, 1228, 1481
 Kleine H, 414, 456
 Klewicki J, 159
 Klimenko AY, 247
 Knaepen B, 991
 Knight DD, 199
 Kolar V, 925
 Kolesnichenko YF, 199
 Komiya A, 394
 Kontis K, 466
 Krogstad PA, 545
 Kronenburg A, 551
 Krumdieck SP, 1026
 Kuo T-C, 1026

 Labraga L, 421
 Lada C, 466
 Lai JCS, 1283

 Lalji F, 1491
 Lanspeary PV, 146, 443, 447, 451
 Lau TCW, 142, 1003
 Laux CO, 594
 Laval JP, 737
 Lavoie P, 287
 Le-Cao K, 659
 Leahy MJ, 112
 Lecoffre Y, 630
 Lee H, 580
 Lee SK, 443, 447, 451
 Leech PW, 527
 Lei C, 117, 121, 125, 368, 398, 402, 406,
 1165
 Leonard E, 328, 1108, 1266
 Levinski O, 129
 Leyland P, 497
 Li C, 531
 Li CG, 68
 Li D, 1108
 Li H, 625, 1038
 Li JD, 903, 980
 Lian Y-Y, 1026
 Lida A, 180, 704, 1295
 Lin W, 699
 Lin WX, 856
 Ling J, 961
 Liovic P, 798
 Liow JL, 866
 Liow KYS, 361
 Liu Y, 1137
 Longmire EK, 135, 744
 Lucey AD, 342, 565, 569
 Lui E, 82

 Mackay D, 1266
 MacLeod JD, 825
 Macrossan MN, 586, 602
 Madan A, 75
 Madawala U, 481
 Madhani JT, 815
 Maeno K, 207
 Magin T, 594
 Mahbub Alam Md, 750
 Mahesh K, 308
 Mai-Duy N, 659, 1321
 Mallon M, 461
 Malpress R, 1258
 Manasseh R, 167, 1328, 1336
 Mandviwalla X, 803
 Manovski P, 677
 Mao Y, 406

Marsh AP, 1213, 1221
 Marusic I, 271, 744, 807, 1436, 1442
 Maruyama S, 394
 Masri AR, 519, 1187, 1344
 Mathis R, 892, 1442
 Mattner TW, 1079
 McBain G, 699
 McCombe C, 786
 McElwain DLS, 616
 McGilvray M, 385
 McGuire JR, 507
 McIntyre T, 594
 McIntyre TJ, 373, 461
 McNeilly IR, 638
 Medwell PR, 1350
 Mee DJ, 491, 645, 1299
 Meland R, 862
 Melatos A, 870
 Meyerer B, 207
 Mi J, 262
 Mirfenderesk H, 233
 Mirzaie H, 671
 Mitchell D, 217
 Mizumo A, 1295
 Mohanamuraly P, 984
 Mohanaragam K, 1405
 Moinuddin KAM, 1254
 Monaghan JJ, 23
 Monty J, 266
 Monty JP, 807, 1436
 Morgan RG, 373, 385, 461, 594, 1177, 1304
 Morgans R, 1432
 Morris-Thomas M, 1091
 Morud JC, 1182
 Moshfegh B, 316
 Mu M, 225
 Mudford NR, 507
 Munipalli J, 1007
 Munkejord ST, 862

 Narasimha M, 1042, 1131
 Naser J, 324, 1411
 Nathan GJ, 262, 447
 Nazarinia M, 1486
 Nedeljkovic M, 876, 881
 Neely AJ, 174, 1309
 Nesic S, 531
 Ng HCH, 807
 Ngan P, 266
 Nickels TB, 271
 Niekamp PN, 1392
 Nielsen O, 939

 Noui-Mehidi MN, 411, 527
 Nydal OJ, 291

 O Neill A, 125
 OByrne A, 456
 OByrne MJ, 954
 OByrne S, 1171
 OFlaherty BT, 295
 Ohmura N, 411
 Olsen R, 862
 ONeill PL, 1123, 1449
 Ooi A, 82, 151, 257, 316, 559, 870, 1063,
 1228, 1328, 1336, 1481
 Ooi ASH, 1436
 Ortiz-Duenas C, 135
 Oza A, 1356
 Ozoe H, 368

 Park G, 1309
 Park GC, 848
 Parker R, 914
 Patterson J, 406
 Patterson JC, 117, 121, 125, 368, 398, 402,
 1165
 Payne EMB, 1336
 Pearce BW, 1399
 Pendrey R, 815
 Pepe RL, 907
 Peralta C, 870
 Periaux J, 471
 Perkins KJ, 241
 Pitman MW, 565, 569
 Please CP, 616
 Poon KW, 870
 Porter JS, 87
 Potter D, 461
 Potter DF, 373
 Prakash M, 1213, 1221
 Pu G, 1415
 Pullinger MG, 94
 Pun CW, 1449

 Qi YQ, 782
 Quaan LM, 667

 Rackemann DW, 1315
 Ran J, 1415
 Ranasinghe R, 939
 Rasul MG, 777, 1050, 1315, 1369
 Razavi SE, 836
 Razzaqi SA, 303
 Reddy KPJ, 32
 Reizes, 1071

Reizes JA, 1108
 Repalle N, 1091
 Resnyansky AD, 1016
 Riboux G, 167
 Ridzwan M, 336
 Risso F, 167
 Roberts MD, 943
 Rottman JW, 947
 Rozakeas PK, 1374
 Rubinsztein-Dunlop H, 461
 Rundstrom D, 316
 Ryan K, 353, 1055, 1457, 1463, 1470

 Saha SC, 117, 121
 Sahoo N, 503
 Saikrishnan N, 744
 Salami A, 976
 Salimi A, 971
 Sankaran R, 1271
 Sargison JE, 87, 94, 241, 819, 1116
 Sato T, 394
 Scarano F, 729
 Schmidt S, 129, 608
 Schultz MP, 907
 Schwarz MP, 112
 Semercigil ES, 1207
 Semercigil SE, 1213, 1221
 Seng OK, 667
 Sengupta TK, 984
 Sexton BA, 527
 Shabani B, 1083
 Shahrokhi A, 475
 Sharifian A, 766
 Sharma M, 385
 Sharma RN, 481, 1242
 Sheard GJ, 353, 1055, 1457, 1463, 1470
 Sheridan J, 1486
 Shervani-Tabar MT, 1420
 Siegenthaler A, 211
 Simonsen A, 1182
 Simonsen AJ, 1154
 Situ R, 815, 848
 Skews BW, 414
 Skvortsov AT, 943
 Smart MK, 303
 Smith BC, 487
 Smith MR, 586
 Smits AJ, 907
 So J, 1457
 Sobbia R, 497
 Song H, 1275

 Soria J, 38, 151, 184, 191, 217, 257, 677,
 712, 726, 737, 892, 1228, 1249, 1475
 Spence CJT, 1364
 Srigrarom S, 336, 1291
 Srinaranyana N, 856
 Srinarayana N, 699
 Srinivas K, 471
 Stalker RJ, 491, 1299
 Stanislas M, 737
 Stappenbelt B, 1491
 Starner S, 519
 Steinberg T, 650
 Stephens DW, 1432
 Strapp JW, 825
 Strunin DV, 720
 Subaschandar N, 638, 1050
 Subic A, 324
 Suman VK, 984
 Sutalo ID, 75

 Tadjfar M, 163
 Tae W, 82
 Tan BT, 361
 Tan G, 1491
 Tan HT, 1291
 Tan MK, 790
 Tan WL, 346
 Tang J, 1020
 Tang X, 531
 Tanimizu K, 1299
 Tao L, 1275
 Tarakemeh N, 786
 Tavner ACR, 1123
 Tetlow GA, 342
 Thiagarajan K, 1007, 1091
 Thiagarajan KP, 1012, 1388
 Thomas IR, 1254
 Thompson MC, 346, 361, 580, 1486
 Thong TB, 667
 Thorpe G, 1193
 Thouas GA, 346, 361
 Tian ZF, 68, 842
 Timchenko V, 1108
 Tio W, 324
 Tomlinson R, 233
 Toophanpour-Rami M, 967
 Tran-Cong T, 659, 1321
 Tseng K-C, 1026
 Tskumamoto Y, 704
 Tsubaki K, 394
 Tu JY, 68, 573, 842, 848, 1405
 Turan OF, 279, 1193, 1207, 1213, 1221